Near-yrast structure of ^{142}Cs and ^{144}Cs

T. Rząca-Urban,[1] J. Genevey,[2] T. Materna,[3] W. Urban,[1,3] A. G. Smith,[4] J. A. Pinston,[2] G. S. Simpson,[2,3] M. P. Sadowski,[1] U. Köster,[3] H. Faust,[3] A. Bail,[5] L. Mathieu,[5] O. Serot,[5] F. Michel-Sendis,[6] and I. Ahmad[7]

[1]*Faculty of Physics, University of Warsaw, ulica Hoża 69, PL-00681 Warsaw, Poland*

[2]*LPSC, Université Joseph Fourier Grenoble 1, CNRS/IN2P3, Institut National Polytechnique de Grenoble, F-38026 Grenoble Cedex, France*

[3]*Institut Laue-Langevin, 6 rue J. Horowitz, F-38042 Grenoble Cedex 9, France*

[4]*Department of Physics and Astronomy, The University of Manchester, M13 9PL Manchester, United Kingdom*

[5]*CEA Cadarache, F-13108 Saint Paul-lez-Durance, France*

[6]*CEA Saclay, F-91191 Gif-sur-Yvette, France*

[7]*Argonne National Laboratory, Argonne, Illinois 60439, USA*

(Received 18 October 2009; published 22 December 2009)

Excited states in ^{142}Cs and ^{144}Cs, populated in the spontaneous fission of ^{248}Cm and ^{252}Cf and in thermal neutron-induced fission of ^{235}U and ^{242}Am were studied by means of γ spectroscopy using the EUROGAM2 and Gammasphere multidetector Ge arrays and the LOHENGRIN fission-fragment separator, respectively. In ^{142}Cs, a band and an isomer with a half-life of $T_{1/2} = 11(3)$ ns have been identified. Spins and parities have been proposed for excited levels in this nucleus. In ^{144}Cs excited levels have been observed. A $T_{1/2} = 1.1(1)$ μs isomer was found with a γ cascade, which probably feeds this isomer. There is also an indication of a nanosecond isomer in ^{144}Cs. Quasiparticle-rotor model calculations done in this work allowed proton-neutron configurations to be proposed for levels in ^{142}Cs and ^{144}Cs.

DOI: 10.1103/PhysRevC.80.064317 PACS number(s): 21.10.Tg, 23.20.Lv, 25.85.Ec, 27.60.+j

I. INTRODUCTION

Odd-odd nuclei provide a natural laboratory to study the coupling between protons and neutrons. However, the structure of odd-odd nuclei is usually rather complex. Therefore, studies of such systems are difficult and their properties are often poorly known. One can obtain new information in this field by investigating the yrast and near-yrast levels in deformed odd-odd nuclei. Such levels usually belong to rotational bands and decay predominantly within the band, producing relatively simple decay spectra. Provided that one has a mechanism to excite such levels, this approach offers a chance to observe and understand at least some proton-neutron excitations in odd-odd nuclei.

The yrast and near-yrast levels in neutron-rich, odd-odd nuclei can be populated up to several units of spin in the fission of actinide nuclei, in which these nuclei are produced as so-called secondary fission fragments (i.e., fission fragments occurring after neutron emission). Such levels can be studied by observing their γ decays. Prompt γ decays can be measured using large arrays of Ge detectors, which have sufficient resolving power to extract and identify individual γ cascades out of the complex radiation pattern emitted by hundreds of different fission products. An alternative and complementary technique is to look for decays of long-lived isomeric states in fission fragments, which, thanks to their long half-lives, can be identified using mass separators. In this work we have used both techniques to study the near-yrast structure of odd-odd cesium isotopes ^{142}Cs and ^{144}Cs.

Section II of this article describes the experiments, the data analysis, and the experimental results. In Sec. III the results are compared to quasiparticle-rotor model calculations, and single-particle configurations are proposed for excited levels. The work is summarized in Sec. IV.

II. EXPERIMENTAL STUDIES OF ^{142,144}Cs

The data from four experiments were used to study ^{142}Cs and ^{144}Cs nuclei; measurements of γ rays following spontaneous fission of ^{248}Cm and ^{252}Cf, performed with the EUROGAM2 and Gammasphere Ge arrays, respectively; and two measurements of delayed γ decays following neutron-induced fission of ^{235}U and ^{242}Am, performed with the LOHENGRIN mass spectrometer at the high-flux reactor of the Institut Laue-Langevin (ILL) Grenoble. The following sections describe these measurements and the respective results.

A. Measurements of γ rays following spontaneous fission of ^{248}Cm and ^{252}Cf

The ^{142}Cs and ^{144}Cs nuclei were populated in spontaneous fission of ^{248}Cm. We observed their γ decays using the EUROGAM2 array of Anti-Compton spectrometers [1]. We also used the data from a measurement of γ rays following spontaneous fission of ^{252}Cf, performed with the Gammasphere array of Anti-Compton Spectrometers at Argonne National Laboratory because timing signals were better in this measurement than in the EUROGAM2 run (see Ref. [2] for more information on the Gammasphere experiment).

In the spontaneous fission of ^{248}Cm, about three neutrons (and no protons) are emitted from fission fragments. Subsequently, prompt γ rays are emitted from both complementary fragments at the same time. Thus, unknown γ cascades in a nucleus of interest can be searched for using the γ-coincidence technique, provided that the complementary fission fragment has known γ decays. High-fold γ coincidences collected with EUROGAM2 were measured and analyzed to determine the excitation schemes of ^{142,144}Cs nuclei. Details of the

TABLE I. Relative intensities of γ transitions in ^{142}Cs, populated in spontaneous fission of ^{248}Cm, as observed in the present work.

E_γ (keV)	I_γ (rel.)	E_γ (keV)	I_γ (rel.)	E_γ (keV)	I_γ (rel.)	E_γ (keV)	I_γ (rel.)
25.3	22(7)	387.5	7(1)	539.2		699.9	10(1)
26.4	51(8)	395.0	10(2)	544.8	33(4)	702.0	4(1)
71.3	18(2)	404.7	71(4)	548.8	15(1)	715.7	11(1)
96.6	47(3)	408.5	43(3)	578.2	2(1)	717.2	4(1)
97.7	35(2)	413.5	7(1)	584.4	3(1)	787.0	3(1)
191.8	14(2)	421.7	0.7(3)	608.8	4(1)	806.8	2(1)
205.3	100(5)	462.3	3(1)	615	2(1)	919.5	2(1)
218.1	62(8)	502.7	5(1)	618.5	12(1)	1060.1	2(1)
327.1	5(1)	537.1	4(1)	678.2	2(1)		

experiment and data analysis techniques were described previously in Refs. [3–5].

1. ^{142}Cs

To search for new levels in ^{142}Cs, we gated on γ lines of ^{103}Nb, the most abundant fission fragment complementary to ^{142}Cs. The excitation scheme of ^{142}Cs obtained in this work is presented in Fig. 1. In Table I we show the relative γ intensities of transitions in ^{142}Cs as observed in the ^{248}Cm fission data.

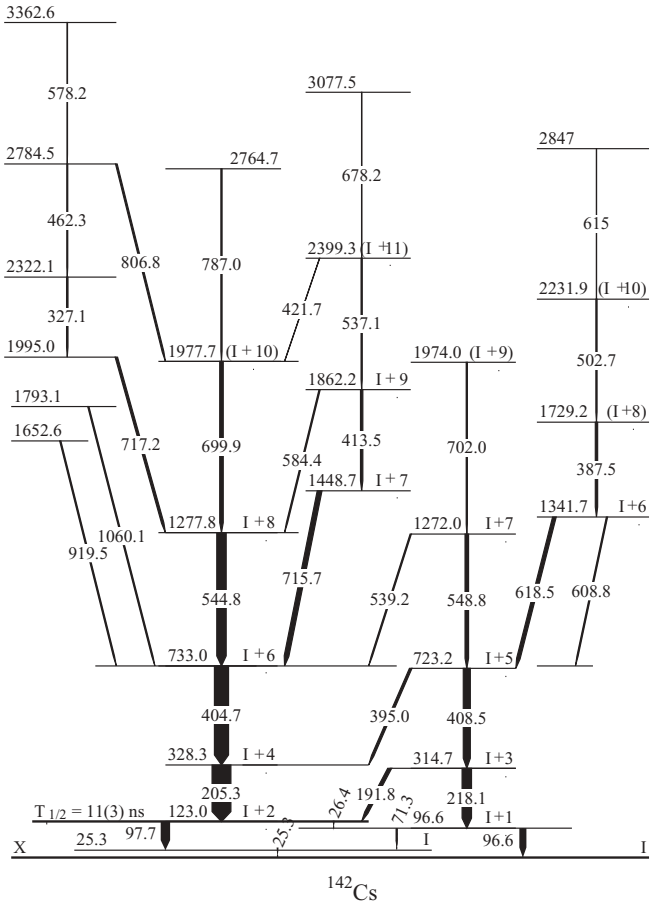

FIG. 1. Excitation scheme of ^{142}Cs as observed in the present work.

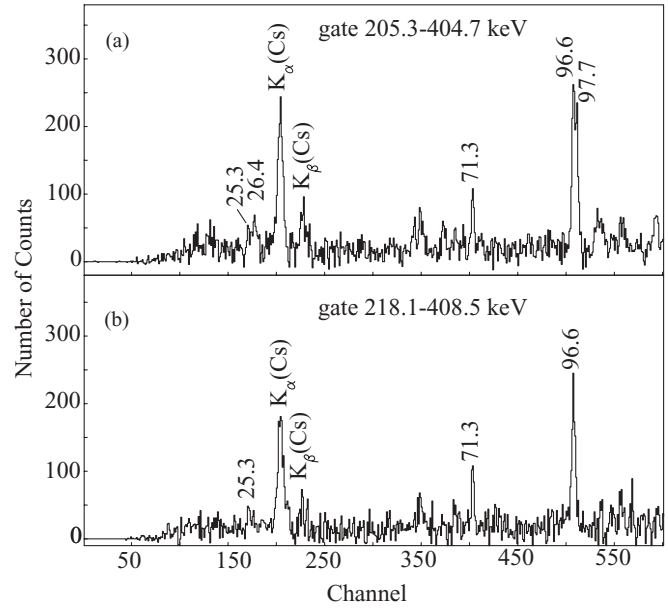

FIG. 2. Low-energy γ-ray spectra from LEPS gated on (a) 205.3- and 404.7-keV lines and (b) 218.1- and 408.5-keV lines in ^{142}Cs. See text for further explanation.

The nucleus ^{142}Cs has been studied before in β^- decay measurements [6], which provide low-spin excitations, and in a measurement of prompt γ rays following fission of ^{252}Cf [7], in which an yrast band was reported extending up to 2.8 MeV. In this article we confirm the cascade of transitions reported in Ref. [7], except for the 2175.8-keV level and the 206.0-keV transition depopulating this level. Seven new transitions (421.7, 462.3, 584.4, 578.2, 678.2, 919.5, and 1060.1 keV) and five new levels (1652.6, 1793.1, 2784.5, 3077.5, and 3362.6 keV) are added to this cascade, as shown in Fig. 1, in the decay scheme of ^{142}Cs obtained in this work.

This scheme has two further additions, as compared to Ref. [7]. First, instead of a single γ line at 97.3 keV reported in [7], we observe two lines at 96.6 and 97.7 keV. The evidence for their presence is shown in Fig. 2(a), which shows a spectrum measured by low-energy photon spectrometers (LEPSs) and doubly gated on the 205.3- and 404.7-keV lines, in which one can observe a double line at 97 keV, with 96.6- and 97.7-keV components of comparable intensity. Figure 2(b) shows a LEPS spectrum doubly gated on the 218.1- and 408.5-keV lines, in which the 96.6-keV line, but not the 97.7-keV line, is observed. Figures 2(a) and 2(b) indicate that the 96.6- and 97.7-keV lines depopulate different levels. The spectra in Fig. 2 show a line at 71.3 keV and in Fig. 2(a) a line at 26.4 keV. The sum of the energies of these two lines agrees with the energy of the 97.7-keV line, suggesting that the 26.4- and 71.3-keV transitions may be located in the scheme parallel to the 97.7-keV transition. Finally, Fig. 2 shows a weak indication of a line at 25.3 keV. Two sums (97.7 + 25.3 keV and 96.6 + 26.4 keV) agree, suggesting the placement of the 25.3 keV transition as shown in Fig. 1.

Second, a new cascade based on the 96.6-keV level is added to the level scheme of ^{142}Cs, as shown in Fig. 1. A fragment of this cascade was reported before as part of the

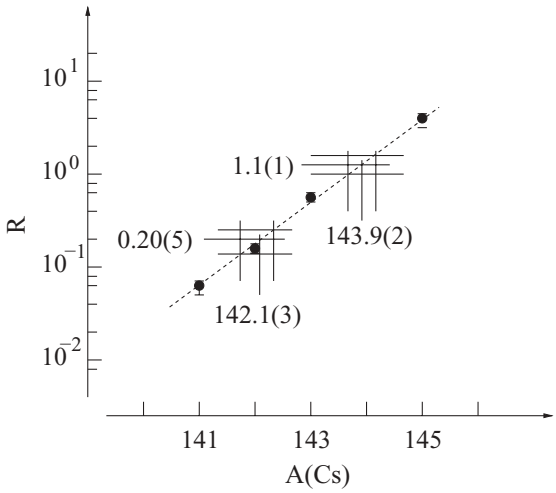

FIG. 3. Mass correlation for Cs isotopes as obtained in this work. See text for further explanation.

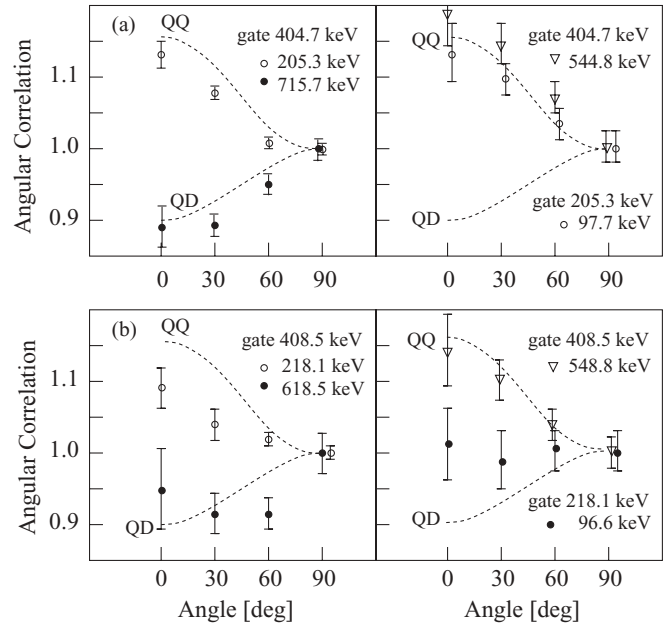

FIG. 4. Angular correlations between rays in ^{142}Cs, as measured in the present work. Q denotes stretched quadrupole and D denotes stretched dipole multipolarity.

excitation scheme of ^{139}Cs [7]; however, as we have shown in our study of ^{139}Cs [8,9], it does not belong to ^{139}Cs. The mass correlation technique proposed in [10] and applied to this band assigns it uniquely to ^{142}Cs, as illustrated in Fig. 3. We applied here a version of this technique presented in Ref. [11]. In Fig. 3 we show, on a logarithmic scale, the ratio of the γ intensity of the 119.4-keV line from ^{101}Nb to the γ intensity of the 126.4-keV line from ^{103}Nb [10], as observed in spectra doubly gated on lines from known bands in ^{141}Cs, ^{142}Cs, ^{143}Cs, and ^{145}Cs isotopes [4,7] (solid dots in the figure). Numerous examples [11–13] show that such a ratio varies smoothly with the mass of the gating cascade, allowing a meaningful interpolation (represented in Fig. 3 by a dashed line). The data for the new cascade are represented by a horizontal bar, which corresponds to the intensity ratio $R = 0.20(5)$. The intersection of this bar with the dashed line determines a mass of 142.1(3) for the isotope to which this cascade belongs. This value indicates clearly that the cascade in question belongs to the ^{142}Cs nucleus.

Compared to Ref. [7], we add to this cascade new transitions of 191.8, 395.0, 539.2, and 608.8 keV, linking this cascade to the cascade based on the 123.0-keV level. This approach confirms the assignment of the new cascade to ^{142}Cs and supports the placement of the 26.4-keV transition from the 123.0-keV level. We also add a new level at 2874 keV.

It could not be determined if the lowest level in Fig. 1 is the ground state of ^{142}Cs, which is known to have spin and parity $I^{\pi} = 0^{-}$. Therefore, it is labeled with energy X and spin I. To deduce the spins of other levels in ^{142}Cs, we measured angular correlations between γ transitions using analysis techniques described in Refs. [14,15]. Figure 4 shows angular correlations for several γ cascades in ^{142}Cs. The correlation between the 205.3- and 404.7-keV lines shown in Fig. 4(a) is consistent with both lines being stretched quadrupoles, whereas the correlation for the 404.7- and 715.7-keV lines indicates a $\Delta I = 1$ character for the 715.7-keV transition. Angular correlations for the 404.7–544.8- and 205.3–97.7-keV cascades, shown in Fig. 4(b), indicate a stretched quadrupole character for the 544.8- and 97.7-keV transitions.

Angular correlations between transitions in the cascade built on top of the 96.6-keV level, shown in Fig. 4(b), suggest a stretched quadrupole character for the 218.1-, 408.5-, and 548.8-keV transitions and a $\Delta I = 1$ character for the 618.5-keV transition. The 96.6-keV transition probably has a mixed $M1 + E2$, $\Delta I = 1$ multipolarity.

We searched for nanosecond isomers in ^{142}Cs using the data from a measurement of γ rays following spontaneous fission of ^{252}Cf, performed with the Gammasphere array. The electronic time windows defining the coincidence events allowed measuring times in a range from -50 to $+900$ ns, counted from time zero given by the "master gate" signal. The time calibration was 0.55 ns per channel and the width of the "prompt" time peak from the Ge detectors was 18 ns—a result of matching the time signal from more than one hundred Ge detectors. The data were sorted into a three-dimensional (3D) histogram, called a *pgt* cube, where we sorted γ signals registered within the prompt time window, extending from -10 to $+10$ ns relative to time zero along the p axis, γ signals with no time restriction on them along the g-axis, and time values corresponding to the g-axis γ signals along the t-axis. From this cube one could obtain clean time spectra for γ transitions by doubly gating on (i) the prompt γ line and (ii) the γ line of interest in coincidence with the prompt line.

A double gating on the 404.7-keV line on the p axis and on the 97.7-keV line on the g axis produced the time spectrum shown in Fig. 5(a). Figure 5(b) shows a prompt time spectrum for the 404.7-keV line (with the first gate set on the 205.3-keV line). The two time spectra are clearly different and suggest that the 97.7-keV line is delayed and the 123.0-keV level may be an isomer in the nanosecond range. In Fig. 5(a) one can also see the so-called jitter effect above channel 500. This effect occurs because of artificially delayed signals produced by the

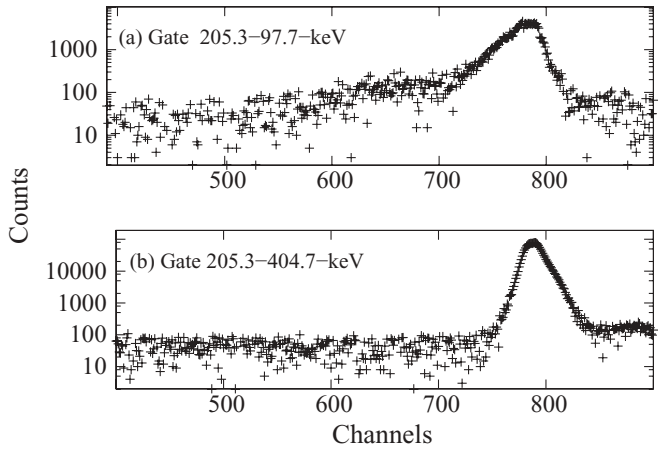

FIG. 5. Time spectra for (a) the 97.7-keV line and (b) the 404.7-keV line in ^{142}Cs.

electronic modules for low-energy γ lines. No jitter is present in Fig. 5(b).

Figure 6 shows a part of the time spectrum of Fig. 5(a) to which we fitted an exponential decay plus constant, obtaining a half-life $T_{1/2} = 11.0(1.5)$ ns [using the shape of the prompt peak from Fig. 5(b) for deconvolution]. Furthermore, we assumed that the jitter effect in the region of the fit is constant and is absorbed into the constant background fit. It may not be exactly the case, but one can see that the jitter is on the level of only a few percent of the isomer intensity. To account for possible systematic uncertainties because of the jitter and the deconvolution procedure, we increased the error on the half-life and adopted the value of $T_{1/2} = 11(3)$ ns for the half-life of the 123.0-keV level in ^{142}Cs.

Considering the quadrupole character of the 97.7-keV transition, the half-life of the 123.0-keV level suggests an $E2$ multipolarity for this transition. This finding may be verified by comparing the partial half-life for the 97.7-keV γ decay of the 123.0-keV level in ^{142}Cs with half-lives of 0.113(5) and 0.068(4) ns for the 2^+ states at 376.8 and 359.5 keV in the ^{140}Xe and ^{142}Ba core nuclei, respectively [16]. The total intensity of the 26.4-keV branch should be equal to the sum of

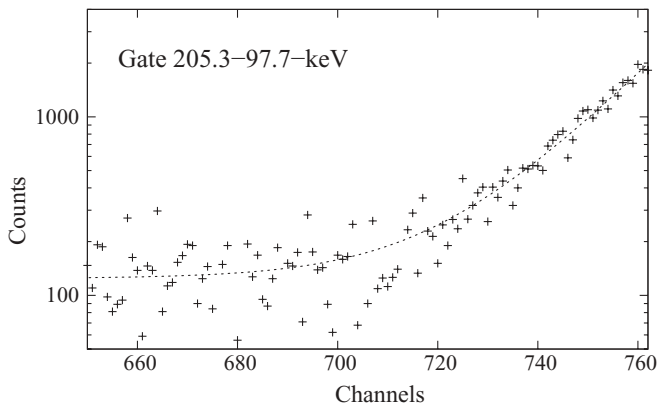

FIG. 6. Time spectrum the 97.7-keV line in ^{142}Cs with an exponential decay plus a constant background fit, represented by the dashed line. Time calibration is 1.1 ns per channel.

intensities of the 71.3- and 96.6-keV transitions, as observed in Fig. 2(a). (These two transitions are easier to analyze than the 26.4-keV transition, especially with respect to internal-conversion contributions.) Taking the intensity of the 97.7-keV line in Fig. 2(a) as 1 arbitrary unit (arb. unit), the γ intensity of the 96.6 keV line is 1.3 arb. units and the γ intensity of the 71.3 keV line is 0.5 arb. unit. Their total intensities are $1.6 < I_{\rm tot}(96.6) < 4.1$ arb. units and $0.8 < I_{\rm tot}(71.3) < 3.8$ arb. units, and the limits are defined by total conversion coefficients for $E1$ and $E2$ multipolarities, respectively. Therefore, the total intensity of the 26.4-keV branch is $2.4 < I_{\rm tot}(26.4) < 7.9$ arb. units, whereas the total intensity of the 97.7-keV branch is 3.03 arb. units, considering $\alpha_{\rm tot} = 2.03$ for an $E2$ transition of 97.7 keV. The total intensity of decays from the 123.0-keV level is then $5.4 < I_{\rm tot}(123.0) < 10.9$ arb. units. Consequently limits for the partial half-life of the 97.7-keV γ branch are $54 < T_{1/2}(97.7) < 153$ ns, which is consistent with the expectation of 81 ns obtained from half-lives in both core nuclei by scaling according to their decay energies and taking an average. For an $M2$ branch of the 97.7-keV transition one would expect a half-life in excess of 10 μs, which allows the $M2$ solution to be rejected.

A time spectrum for the 96.6-keV line does not show any clear evidence of a lifetime. This observation and the angular correlation for this line shown in Fig. 4 indicate that the 96.6-keV transition is not a stretched quadrupole. Therefore, we propose spin $I + 1$ for the 96.6 keV level (assuming that spins are growing with increasing energy as is commonly observed in nuclei populated in fission). Consequently the spin of the 123.0-keV level should be $I + 2$, because it cannot be higher because of the presence of the low-energy 26.4-keV decay, yet it cannot be lower because of the nonobservation of a 123.0-keV decay to level X. The $I + 2$ spin assignment to the 123.0-keV level implies spin I for the 25.3-keV level. Angular correlation data obtained above suggest spins of higher energy levels as shown in Fig. 1.

The close proximity of the X and 25.3-keV levels, both having the same spin, suggests that they have opposite parities and the 25.3-keV transition has an $E1$ multipolarity. Consequently, the 123.0-keV level has a parity opposite that of the parity of level X. This finding is consistent with the nonobservation of the 123.0-keV transition, which should in this case have an $M2$ multipolarity. If the parities were the same one would expect an $E2$ transition of 123.0 keV from the 123.0-keV level.

Finally, a number of weak arguments suggest that the 96.6-keV level has the same parity as the level X. First is the angular correlation for the 96.6-keV line, as mentioned earlier. Second is the balance between the total feeding and decay intensities of 123.0-, 96.6-, and 25.3-keV levels. The best agreement is obtained if the 26.4- and 71.3-keV transitions are both $E1$ in character.

The nonobservation of any decay from the level X in our data means that this level is either the ground state or a low-lying state with a long half-life. Interestingly, no overlap occurs between our level scheme and the excitation scheme observed in β^- decay of the 0^+ ground state of ^{142}Xe [6]. Such a decay populates only nonyrast excited levels with low spins. Nevertheless, levels with spins $I \leqslant 2$ should be observed. The

lack of any overlap between the two measurements is against the hypothesis that the level X is the ground state, because in that case at least the 25.3- and 96.6-keV levels should be seen in β^- decay. The level X may be identical with the level at 12.8 keV reported in β^- decay [6], although in this case our 25.3-keV levels should be seen in the β^--decay measurement at 38.1 keV, which is not reported in Ref. [6]. Any of the higher energy levels observed in β^- decay cannot correspond to our level X because these levels decay through transitions with energies high enough to be observed in our data. It is likely that the level X is a long-lived isomer with spin $I \geqslant 2$.

2. ^{144}Cs

No excited levels in the ^{144}Cs nucleus have been reported to date, although it has been pointed out that an isomeric state may exist at low excitation energy [17]. We have searched for prompt γ lines in ^{144}Cs by gating on known γ lines in ^{101}Nb [10] using our ^{248}Cm fission data. A new cascade of γ transitions has been found, all of which are in prompt coincidence with lines in both ^{101}Nb and ^{103}Nb nuclei. Therefore, the cascade belongs to a cesium isotope. The ratio of the γ intensity of the 119.4 keV line from ^{101}Nb to the γ intensity of the 126.4 keV line from ^{103}Nb, $R = 1.1(1)$, found in the spectrum doubly gated on lines from the new cascade, uniquely assigns the new cascade to the ^{144}Cs nucleus, as illustrated in Fig. 3.

Figure 7 shows the proposed partial-level scheme of ^{144}Cs consisting of a prompt γ cascade obtained from the ^{248}Cm fission data and an isomeric cascade observed in neutron-induced fission of ^{235}U, as discussed in the next section. The prompt γ cascade ends at level X, which may be identical to the 1.1 μs isomer at 92 keV found in neutron-induced fission; however, it may also be another isomer or even the ground state.

Table II shows the relative intensities of γ rays in ^{144}Cs populated in fission of ^{248}Cm and observed in this work.

Angular correlations between transitions in the new cascade were determined, as shown in Fig. 8. They are limited to the lowest-lying transitions because of the low intensity of the cascade. The data show that the 107.9- and 114.6-keV transitions are consistent with a mixed $M1 + E2$, $\Delta I = 1$ multipolarity, and the 263.3- and 404.7-keV transitions are consistent with a stretched quadrupole ($E2$) multipolarity. A regular energy increase suggests that a rotational band on top of the level with spin $I + 2$ can be observed, where spin I is assigned to level X.

We have checked for the presence of nanosecond isomers in ^{144}Cs using the ^{252}Cf fission data. A fragment of a spectrum

TABLE II. Relative intensities of γ transitions in ^{144}Cs, populated in spontaneous fission of ^{248}Cm.

E_γ (keV)	I_γ (rel.)	E_γ (keV)	I_γ (rel.)	E_γ (keV)	I_γ (rel.)	E_γ (keV)	I_γ (rel.)
107.9	100(5)	263.3	48(4)	473.8	35(4)	565.0	5(1)
114.6	99(6)	404.7	39(3)	535.1	12(2)		

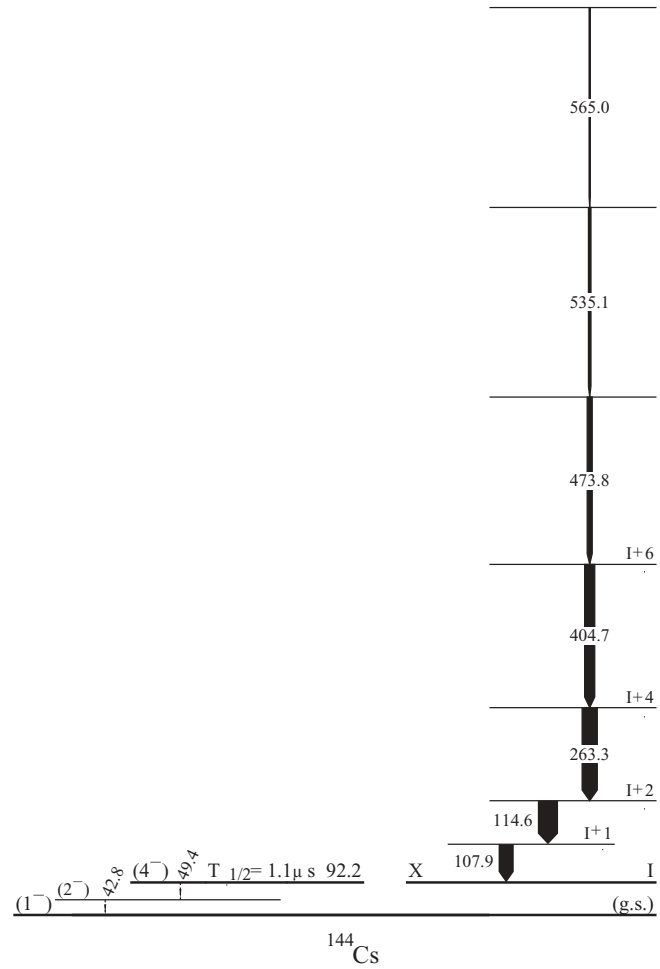

FIG. 7. Level scheme of ^{144}Cs as observed in the present work.

doubly gated in the pgt cube with the p-axis gate set on the 263.4-keV line and the g-axis gate set on the 107.9-keV line is shown in Fig. 9(a). For comparison, Fig. 9(b) shows an analogous time spectrum for the 404.7-keV line. Some difference exists between slopes of prompt peaks shown in Figs. 9(a) and 9(b), suggesting that the 107.9-keV line may be the decay of a nanosecond isomer. No noticeable effect was found for the 114.6-keV line.

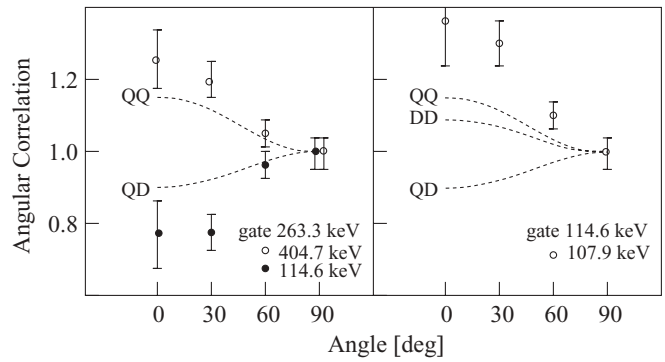

FIG. 8. Angular correlations between rays in ^{144}Cs as measured in the present work. Q denotes a stretched quadrupole and D a stretched dipole multipolarity.

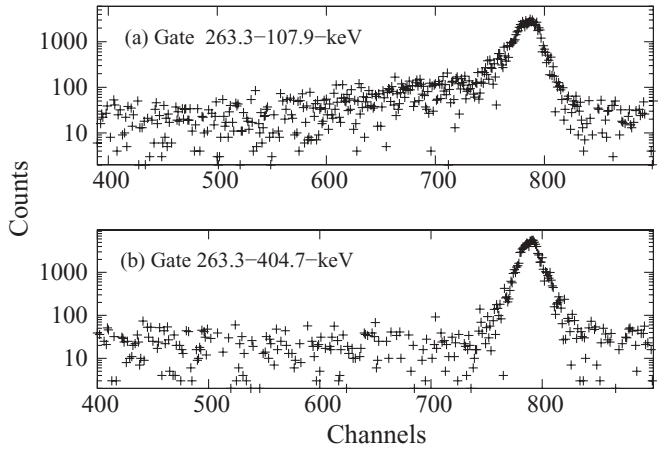

FIG. 9. Time spectrum of (a) the 107.9-keV and (b) the 404.7-keV lines in ^{144}Cs. Time calibration is 1.1 ns per channel.

The usual fitting procedure with unfolding produces a large error, which should still be increased considering the possible systematic errors as discussed earlier. Therefore, we provide an upper limit of $T_{1/2} \leqslant 8$ ns for the half-life of the $(X + 107.9)$-keV level only.

B. Measurement of delayed γ rays following neutron-induced fission of ^{235}U

The half-life of the $(X + 107.9)$-keV level in ^{144}Cs is at the limit of what can be measured using our ^{252}Cf fission data. Therefore, we applied another technique to verify the presence of nanosecond isomers proposed in ^{142}Cs and ^{144}Cs.

A search for nanosecond isomers in ^{142}Cs and ^{144}Cs was performed at the LOHENGRIN fission-fragment separator [18] using the method proposed in [19]. Both nuclei were populated in neutron-induced fission of ^{235}U. The ^{235}U target was placed close to the core of the ILL reactor in a neutron flux of 5×10^{14} $n/(\mathrm{s\ cm}^2)$. The target was prepared in the form of a 206 $\mu\mathrm{g/cm}^2$ layer of UO_2 on a Ti backing, covered with a 0.25-μm Ni foil. The distance between the target and the foil was less than 0.3 mm and the foil was thin enough for fission fragments of about 60 MeV kinetic energy to easily fly out of the target. During the fragment's passage of the nickel foil the ionic charge of the fragment, q, is established by an equilibrium between stripping and electron capture. The charge distribution is approximately a Gaussian [20] centered at $q \approx 21$ for fragments with mass around $A = 140$. These, so-called secondary fission fragments (i.e., fission fragment nuclei after neutron emission) were then analyzed by LOHENGRIN according to the q/m ratio (where m denotes the mass of an ion) and collected on a thin plastic tape placed between two Clover Ge detectors [21] in close geometry, which measured γ rays following β^- decays of implanted ions. These E_γ uniquely identified individual "parent" nuclei out of a few different masses m arriving at the implantation point. The tape was moved periodically to reduce the activity from subsequent β^- decays in the mass chain of interest. A more detailed description of this measurement can be found in Ref. [22].

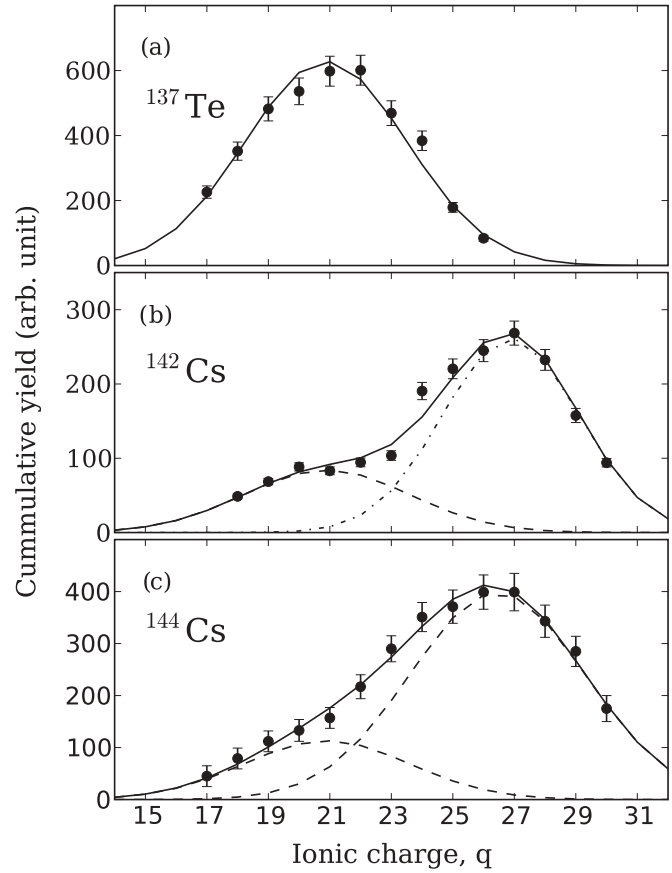

FIG. 10. Ionic charge distributions for (a) ^{137}Te, (b) ^{142}Cs, and (c) ^{144}Cs. In (a) a single Gaussian and in (b) and (c) two Gaussian shapes are fitted to data points. See text for further explanation.

We measured the intensity of γ rays corresponding to a β^- decay of a given parent nucleus for different q values selected by LOHENGRIN. Figure 10 shows these charge distributions obtained for ^{137}Te, ^{142}Cs, and ^{144}Cs fission fragments arriving at the collection point.

Clear differences exist among the charge distributions for the three nuclei. For ^{137}Te the distribution has a shape of a single Gaussian centered at $q \approx 21$, whereas the charge distributions for ^{142}Cs and ^{144}Cs ions peak at higher values of q and have more complex shapes. This effect was explained in Ref. [19] as being caused by a decay of isomeric states in secondary fission fragments after they pass the (nickel) foil covering the target, where the charge equilibrium is established. If such a decay proceeds via a strongly converted, low-energy transition bearing a significant fraction of the total decay intensity (i.e., located at the bottom of a decay scheme), an emission of the conversion electron and the following Auger electrons increases the ionic charge by a few units. If this happens before the ion enters the analyzing magnet of LOHENGRIN, then at the exit of the separator one observes the initial charge distribution produced in the foil covering the target with a centroid shifted toward a higher charge.

With a single Gaussian curve fitted to the charge distribution for ^{137}Te we obtained a good reproduction of the data, with the center of the distribution at $q \approx 21$ as shown in Fig. 10(a).

We conclude that in this case no isomeric decay is present, in accord with the excitation scheme observed in our earlier work [23].

Two Gaussian curves were fitted to the charge distributions for ^{142}Cs and ^{144}Cs and are shown in Figs. 10(b) and 10(c), respectively. A good reproduction of the data was obtained in both cases with one Gaussian centered at $q \approx 21$, as observed in ^{137}Te, and the other at $q \approx 27$. These results indicate the existence of nanosecond isomers in both Cs isotopes.

In the case of ^{142}Cs and ^{144}Cs, the ratio of integrals under the two Gaussian peaks shown in Figs. 10(b) and 10(c) bears information about the half-lives of isomers in these nuclei. However, the peak at $q = 21$ may be either because of a partial decay of the isomer before passing the foil or because of a prompt decay to the ground state, bypassing the isomer. In the case of ^{142}Cs this would result in either a partial isomeric decay of the 123.0-keV level before the ion passes through the foil or a prompt decay of the 96.6-keV level (see Fig. 1). Therefore, such a measurement is not sufficient for a half-life determination. Further measurements are being prepared in subsequent work using two Ni foils where the second foil is placed a few centimeters behind the first one, which should resolve this problem [22].

The results obtained here for ^{142}Cs and ^{144}Cs are consistent with the data obtained from fission of ^{252}Cf and confirm the presence of nanosecond isomers in these two Cs isotopes.

C. Measurement of delayed γ rays following neutron-induced fission of ^{242}Am

A cascade of two low-energy transitions of 42.8 and 49.4 keV was found to de-excite a new isomeric level in ^{144}Cs, which has a half-life of $T_{1/2} = 1.1(1)$ μs.

Fission fragments of the $A = 144$ mass chain were produced by thermal neutron-induced fission of $^{242g+m}$Am that was bred from a ^{241}Am target in the high neutron flux at the LOHENGRIN target position. The LOHENGRIN spectrometer has been used to separate fission fragments of ionic charge $q = 22$ recoiling from a thin target of about 870 μg/cm^2. The fragments were detected in an ionization chamber filled with isobutane gas. This chamber consists of two regions of gas, $\Delta 1 = 9$ cm and $\Delta 2 = 6$ cm in length. A 6-μm-thick mylar foil was placed at the end of the chamber. The γ decays from isomeric states were detected by two Clover Ge detectors [21] and the conversion electrons were detected by two cooled Si(Li) detectors covering a total area of 2×6 cm^2 and located 7 mm behind the mylar foil. The gas pressure of the ionization chamber was adjusted to stop fission fragments at about 2 μm from the surface of the mylar window to minimize the absorption of conversion electrons to maintain a good energy resolution. The flight time of the $A = 144$ fission fragments through LOHENGRIN was about 2 μs. After the arrival of an ion at the mylar foil, γ rays and electrons were detected in the Ge and Si detectors, respectively, in a time window of 20 μs. More information about the chamber properties and measurements of microsecond isomers can be found in Refs. [24,25].

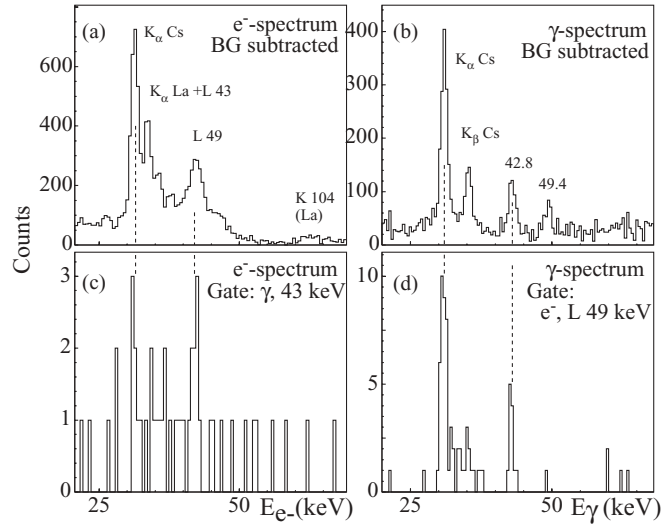

FIG. 11. (a) Electron and (b) γ spectra of the $A = 144$ mass chain in delayed coincidence with the fission fragments, (c) electron spectrum gated on the 43-keV γ line, and (d) γ spectrum gated by the L 49-keV electron transition.

The electron and γ spectra measured in delayed coincidences with fission fragments of the $A = 144$ mass chain are shown in Figs. 11(a) and 11(b). Two new γ decays of 42.8 and 49.4 keV have been observed. Both lines are clearly seen in the γ spectrum in Fig. 11(b). In the electron spectrum in Fig. 11(a), the L 49-keV electron line is also clearly seen. The x rays of lanthanum, which are attributed to the β decay of ^{144}Ba, are still present after background substraction, overlap with the L 43-keV line.

The two lines are in a cascade, as illustrated in Figs. 11(c) and 11(d). Figure 11(d) shows a γ spectrum in coincidence with the L 49-keV electron line. The 42.8-keV γ line is clearly coincident with the 49-keV electron line; the latter is also in strong coincidence with cesium K x rays. The two lines define a new level at 92.2 keV, as shown in Fig. 7.

Because the 42.8- and 49.4-keV decays were observed in a period starting about 2 μs after the population of the 92.2-keV level in the target, their detection indicates that the 92.2-keV level is an isomer. We measured the time-decay spectrum corresponding to the 49.4-keV γ line in a time window of 20 μs started by the arrival of an ion. An exponential-decay plus constant-background function fitted to the relevant part of the spectrum, as shown in Fig. 12, yields a half-life of $T_{1/2} = 1.1(1)$ μs for the 92.2-keV level.

Our estimates of experimental conversion coefficients for the two lines in the isomeric cascade are not precise because of experimental limitations. The γ intensity of the 49.4-keV line could not be measured precisely because of its low intensity and a contamination by the 50-keV line belonging to ^{131}Sb, which, because of its similar m/q value, is also present in the data. The L 43-keV line is covered by the La x-ray lines and also could not be evaluated. Nevertheless, the coefficient $\alpha_L = 10(4)$, estimated for the 49.4-keV transition, is compatible with an $E2$ assignment only. The α_L value of the 42.8-keV transition should be lower than that of the 49.4-keV transition due to its higher γ intensity, as seen

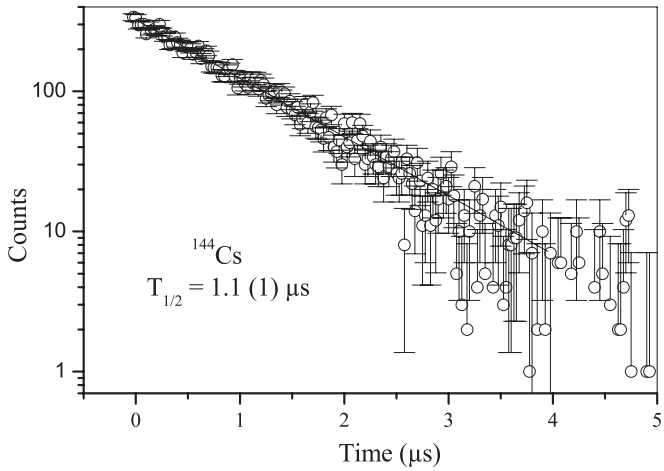

FIG. 12. A time spectrum for the 49.4-keV transition in ^{144}Cs corresponding to the decay of the 1.1(1) μs isomer in ^{144}Cs, as observed in fission of ^{235}U + $n_{\rm th}$ in this work. The time scale is 100 ns/channel. The dashed line represents an exponential-decay plus constant-background fit to the data.

in Fig. 11(b). The ratio of the K x-ray intensity to the γ intensity of the 42.8-keV line, $I(X)/\gamma \approx 7$, as observed in the spectrum gated on the L 49-keV line in Fig. 11(d), makes either an $M1$ or an $E2$ assignment possible for the 42.8-keV transition. However, the $I(X)$ intensity in Fig. 11(d) also contains a contribution from the conversion of the 49.4-keV line. Therefore, the $I(X)/\gamma$ value for the 42.8-keV line should be lower than the aforementioned estimate. Moreover, an $E2$ assignment implies a theoretical coefficient $\alpha_L = 25$, which is higher than the α_L value found for the 49.4-keV transition and contradicts our previous conclusion. Therefore, we exclude a pure $E2$ assignment for the 42.8-keV transition. A multipolarity assignment of $M1$ with a small admixture of $E2$ for the 42.8-keV transition is consistent with the intensity balance for the 49.4-keV transitions.

One may thus conclude that the new $T_{1/2} = 1.1$ μs isomer observed in the ^{144}Cs nucleus decays by a stretched $E2$, isomeric transition of 49.4 keV, in good agreement with the Weisskopf estimate, followed by an $M1 + E2$ transition. The latter should correspond to a $\Delta I = 1$ spin change because, in the case of a $\Delta I = 0$ spin change, an $E2$ isomeric transition of 92.2 keV should be observed. Consequently, the spin and parity of the 42.8-keV level is 2^- and spin and parity of the 92.2-keV isomer is 4^-, assuming that the isomeric cascade directly feeds the ground state, for which we took spin and parity 1^- from the literature [17].

III. INTERPRETATION OF EXCITED LEVELS IN ^{142,144}Cs

An unknown isomer in ^{144}Cs, having spin $I = 4$ or higher, was mentioned in the Nuclear Data compilation [17]. The odd-proton nucleus ^{143}Cs was assigned spin-parity $3/2^+$ in its ground state [4,26] whereas the odd-neutron nucleus ^{143}Xe was assigned spin-parity $5/2^-$ in the ground state [27]. Therefore, for the ground state and the low-energy excited levels in ^{144}Cs, one expects a negative parity and spins from $I = 1$ to $I = 4$, resulting from this proton-neutron coupling. It is likely that the ground state and the excited levels at 42.8 and 92.2 keV in ^{144}Cs are the 1^-, 2^-, and 4^- members of the $(\pi^+_{3/2}[422] \times \nu^-_{5/2}[523])_j$ configuration, respectively.

We note that two low-lying levels exist in ^{143}Cs at 76.5 and 90.4 keV, which were assigned spin-parities of $5/2^+$ and $7/2^+$, respectively. They are strongly linked to each other and to the ground state [26]. One may thus expect two low-lying levels in ^{144}Cs with spins 5^- and 6^-, the latter being a bandhead analogous to the $7/2^+$ bandhead in ^{143}Cs. Therefore, the probable scenario for ^{144}Cs is that the microsecond isomer and the level X is the same level at 92.2 keV with spin and parity 4^- and there is a bandhead at 314.7 keV with spin and parity $I^\pi = 6^-$ and a rotational band on top of it.

To obtain more insight into the structure of the ^{144}Cs nucleus, we performed calculations within the framework of the quasiparticle rotor model (QPRM) using the codes GAMPN, ASYRMO, and PROBI [31]. In the calculations we used a deformation of $\epsilon_2 = 0.16$, as deduced from the measured value of $Q_s = 0.30(1)$ b [32] and a Coriolis attenuation parameter of $\xi = 0.95$. Standard values for the κ and μ parameters of the ls and l^2 terms were used [33]. More information on such calculations can be found in Refs. [34] and [35].

We note that, because of the low deformation of ^{144}Cs, the validity of the Nilsson model is at its limit in this nucleus and one should expect only some guidance from such calculations rather than any exact reproduction of the experimental data. It is also worth noting that for odd-A Cs isotopes octupole deformation has been predicted in their ground states [36], explaining the reversed order of the 1/2[530] and 3/2[532] proton orbitals compared to the prediction of the Nilsson model. However, our work on ^{141,143,145}Cs isotopes have shown that in excited states of these nuclei octupole correlations are weak [26,37], which may justify the use of the Nilsson model with a reflection-symmetric potential.

The results of our calculations for ^{144}Cs are compared in Fig. 13 with the experimental data. In this figure we assumed that the level X from Fig. 7 has an excitation energy of 92.2 keV and spin and parity $I^\pi = 4^-$. Consequently, higher experimental levels have energies and spins as shown in Fig. 13.

In the weakly deformed ^{144}Cs nucleus, many proton-neutron Nilsson orbitals are located close to each other. Quasiparticle proton and neutron dominating configurations, which are close to the Fermi surface in ^{144}Cs, are shown in the inset in Fig. 13. These are $\Omega = 1/2$ and $\Omega = 3/2$ Nilsson subshells, originating from $g_{7/2}$ and $d_{5/2}$ spherical shells for protons, labeled A and B, respectively, and $\Omega = 1/2$, $\Omega = 3/2$, and $\Omega = 5/2$ Nilsson subshells, originating from $f_{7/2}$ and $h_{9/2}$ spherical shells for neutrons and labeled C, D, and E, respectively, in Fig. 13. The subshells with the same Ω value are mixed and, consequently, may produce multiple proton-neutron excitations in ^{144}Cs of the same spin at comparable energies. Therefore, in addition to excitation energies, other characteristic features of levels, such as electromagnetic moments, should be used to identify correct solutions. For the ground state the electric moment, $Q = 0.30(1)$ b, and magnetic moment, $\mu = -0.546(3)\mu_N$, were reported [32] and in the

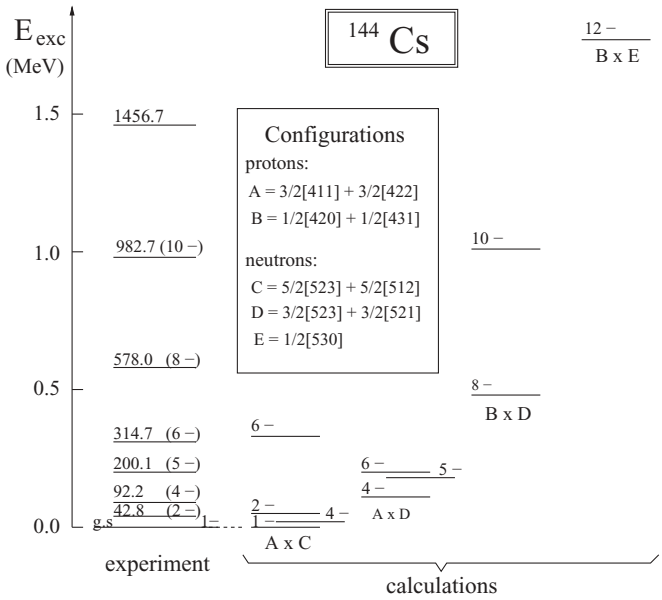

FIG. 13. Comparison of the experimental and calculated energies of excited states in ^{144}Cs obtained in the present work.

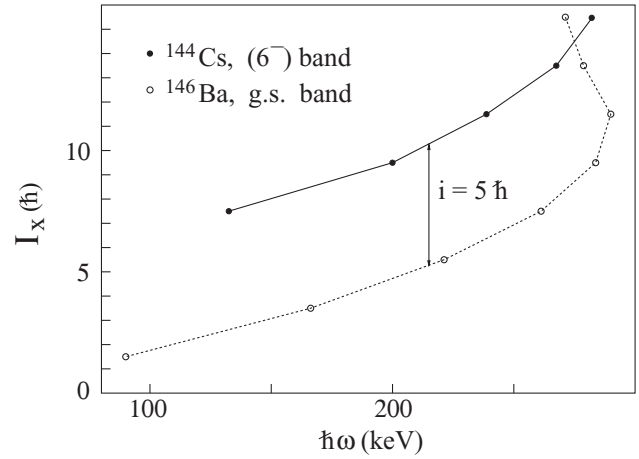

FIG. 14. Spin alignments in the (6^-) band of ^{144}Cs and in the ground-state band of ^{146}Ba.

present work we have found a half-life for the 92.2-keV level, $T = 1.1(1)$ μs. Considering the ground-state spins of ^{143}Cs and ^{143}Xe, one also expects that the ground state of ^{144}Cs should have the spin projection quantum number $K = 1$.

There is only one solution with spin 1^- and $K = 1$, labeled A × C in Fig. 13, which reproduces the experimental electric and magnetic moments for the ground state, providing calculated values of $Q_{\rm th} = 0.271$ b and $\mu_{\rm th} = -0.567\mu_N$, respectively. We propose that this solution corresponds to the ground state in ^{144}Cs. In Fig. 13, this calculated 1^- level of the A × C configuration is placed at zero energy and all other calculated levels are drawn relative to this level. It should be noted that this level appears in the calculations about 100 keV above the lowest calculated level, which corresponds to the A × D configuration and also has spin and parity 1^-. However, it has $K = 0$ and does not reproduce the electromagnetic moments of the experimental ground state.

The 42.8-keV first excited state with spin 2^- and $K = 1$ and the 314.7-keV excited state with spin 6^- and $K = 4$ are reproduced well by the A × C coupling. However, the 4^- member of the A × C multiplet (with $K = 4$) appears too low in energy. For the 92.2-keV isomer, the A × D coupling with $K = 3$ may be proposed, for which the calculated half-life amounts to 3.1 μs, which is in fair agreement with the measured value. The A × D configuration provides a good description for the (5^-) level at 200.1 keV and there is also a low-lying 6^- solution in this coupling, which may be considered for the 314.7-keV (6^-) level instead of the A × C solution. The band on top of the (6^-) level may be interpreted as the $(d_{5/2}, f_{7/2})$ or $(d_{5/2}, h_{9/2})$ proton-neutron aligned configuration. The $(d_{5/2}, f_{7/2})$ solution is preferred, because its favored branch has even spins. We note that characteristic, low-lying 6^- levels have been observed in the nearby odd-odd nuclei ^{138}Cs [29] and ^{138}I [30], and they were interpreted as owing to the $(\pi d_{5/2}\nu f_{7/2})_{6^-}$ spherical configuration.

The proposed interpretation of the band on top of the (6^-) level is supported by the spin alignment seen in this band, as displayed in Fig. 14. Relative to the ground-state band in ^{146}Ba, the proposed (6^-) band has an aligned angular momentum of $5\hbar$, which is consistent with an alignment that can be produced by the $d_{5/2}$ proton and the $f_{7/2}$ or $h_{9/2}$ neutrons. This observation is important because one may also think of other proton-neutron configurations involving the intruder $i_{13/2}$ neutron orbital. With increasing neutron number, this orbital lowers its energy and in ^{145}Cs the $13/2^+$ excitation, with the dominating $\nu i_{13/2}$ component, is observed at 607 keV [37]. However, there the $\nu i_{13/2}$ orbital alone aligns $5.5\hbar$ of angular momentum [37]. Therefore, the proposition that the yrast band in ^{144}Cs may involve the $\nu i_{13/2}$ orbital is less likely. In such a case, the discussed bandhead in ^{144}Cs should be expected at an excitation energy higher than 315 keV and having spin higher than $6\hbar$ as well as positive parity.

For higher spin levels in the yrast band of ^{144}Cs, the calculations favor the B × D solution for the (8^-) level at 578.0 keV and the (10^-) level at 982.7 keV, which are clearly yrast in the calculations. The B × E configuration provides an yrast 12^- solution, which may correspond to the 1456.7-keV experimental level. The irregular energy increase in the yrast band of ^{144}Cs justifies such configuration changes within this band.

We have not performed any calculations for ^{142}Cs because the deformation of this nucleus is even lower than the deformation of ^{144}Cs, limiting the use of the QPRM. However, ^{142}Cs is too collective for the shell model calculations, which are still applicable for the ^{138}Cs nucleus [29]. Instead, we provide some general comments that may help in understanding the near-yrast structure of ^{142}Cs.

The ^{142}Cs isotope with $N = 87$ is a complex transitional nucleus. For odd-A Cs isotopes with $N < 87$, one observes spherical ground states with spin $I^\pi = 7/2^+$, corresponding to the $g_{7/2}$ proton orbital, and for isotopes with $N > 87$, one observes deformed ground states with spin $I^\pi = 3/2^+$, corresponding to a (deformed) 3/2[422] Nilsson orbital originating from the $g_{7/2}$ spherical proton orbit. The change

from a spherical to a deformed shape in Cs isotopes takes place at $N = 87$. The situation is different in the chain of Xe isotopes, where the ^{137}Xe nucleus has a spherical ground state with spin $7/2^-$ but ^{139}Xe has the ground state with spin $3/2^-$, which corresponds to a Nilsson orbital. This would indicate a shape transition in Xe isotopes already at $N = 85$. The additional collectivity in Xe, as compared to Cs, may be due to octupole correlations [28].

For the low-energy levels in ^{142}Cs one expects spins and parities resulting from coupling of the $7/2^+$ proton ground state in ^{141}Cs [4,26] to the $5/2^-$ neutron ground state in ^{141}Xe [27,28]. The parity resulting from this coupling is negative whereas spin values may vary from $I = 1$ to $I = 6$. The 0^- spin-parity assignment reported for the ground state of ^{142}Cs [6] does not match this expectation. However, there is a low-lying $5/2^+$ excited level at 105.7 keV in ^{141}Cs [26], which may form an $I^\pi = 0^-$ ground state in ^{142}Cs by coupling to the $5/2^-$ ground state in ^{141}Xe. Alternatively, it is possible that a low-lying $7/2^-$ state at 35.6 keV in ^{141}Xe [28] forms the 0^- ground state in ^{142}Cs by coupling to the $7/2^+$ ground state in ^{141}Cs. While the first solution would provide a deformed state, the second solution should correspond to a spherical shape. Measurements of Q and μ electromagnetic moments may help in deciding which solution is correct.

It is not obvious what the spin and parity of the level labeled X in Fig. 1 should be. One may argue that the bandhead seen at 123.0 keV in Fig. 1 corresponds to a maximum-aligned configuration $\pi d_{7/2}\nu f_{7/2_{6^-}}$ or $\pi g_{7/2}\nu f_{7/2_{7^-}}$, as observed in the neighboring odd-odd Cs and I isotopes. Considering the discussion of spin-parity assignments in ^{142}Cs presented in Sec. II A1, where we concluded that the level X has the same parity as the 123.0-keV level and spin lower by two units, one may propose spin and parity of 4^- or 5^- for the level X. Such a solution would be similar to the situation in ^{144}Cs and may imply the existence of one or two isomers in the micro- to millisecond range, which so far have escaped detection. It is also possible that such an isomer (isomers) could have a β^--decay branch not observed before. We note that spin $I^\pi = 4^+$ is populated in ^{142}Ba in β^- decay of ^{142}Cs [6]. It is worth verifying if this happens via γ cascades following β^- decay of the 0^- ground state in ^{142}Cs or if the $I^\pi = 4^+$ level in ^{142}Ba is populated directly in β^- decay of ^{142}Cs. The latter would indicate the existence of a long-lived isomer in ^{142}Cs.

IV. SUMMARY

Medium spin excitations in the ^{142}Cs and ^{144}Cs nuclei, populated in the spontaneous fission of ^{248}Cm and ^{252}Cf and in the neutron-induced fission of ^{235}U and ^{242}Am, have been studied experimentally using the EUROGAM2 and Gammasphere multidetector arrays and the LOHENGRIN mass separator. In ^{142}Cs we have found a yrast band and proposed a structure at low spins, including an 11(3) ns isomer. In ^{144}Cs we have observed excited states and identified a 1.1(1)-μs isomer, for which spin $I^\pi = 4^-$ has been proposed. For the ^{144}Cs nucleus, we performed QPRM calculations, proposing multiparticle configurations for the ground state, for the 1.1-μs isomer, and for the (6^-) bandhead. The lowest level observed in ^{142}Cs in this work may be a long-lived (micro- to millisecond) isomer with spin 4^- or 5^-.

ACKNOWLEDGMENTS

This work was partly supported by the US Department of Energy, Office of Nuclear Physics, under Contract No. DE-AC02-06CH11357. The authors are indebted to the Office of Basic Energy Sciences, US Department of Energy, for the use of ^{248}Cm through the transplutonium element production facilities at the Oak Ridge National Laboratory.

[1] P. J. Nolan, F. A. Beck, and D. B. Fossan, Annu. Rev. Nucl. Part. Sci. **44**, 561 (1994).
[2] D. Patel, A. G. Smith, G. S. Simpson, R. M. Wall, J. F. Smith, O. J. Onakanmi, I. Ahmad, J. P. Greene, M. P. Carpenter, T. Lauritsen, C. J. Lister, R. V. F. Janssens, F. G. Kondev, D. Seweryniak, B. J. P. Gall, O. Dorveaux, and B. Roux, J. Phys. G **28**, 649 (2002).
[3] W. Urban, M. A. Jones, C. J. Pearson, I. Ahmad, M. Bentaleb, J. L. Durell, M. J. Leddy, E. Lubkiewicz, L. R. Morss, W. R. Phillips, N. Schulz, A. G. Smith, and B. J. Varley, Nucl. Instrum. Methods **365**, 596 (1995).
[4] T. Rząca-Urban, W. R. Phillips, J. L. Durell, W. Urban, B. J. Varley, C. J. Pearson, J. A. Shannon, I. Ahmad, C. J. Lister, L. R. Morss, K. L. Nash, C. W. Williams, M. Bentaleb, E. Lubkiewicz, and N. Schulz, Phys. Lett. **B348**, 336 (1995).
[5] W. Urban, J. L. Durell, W. R. Phillips, A. G. Smith, M. A. Jones, I. Ahmad, A. R. Barnet, S. J. Dorning, M. J. Leddy, E. Lubkiewicz, L. R. Morss, T. Rząca-Urban, R. A. Sareen, N. Schulz, and B. J. Varley, Z. Phys. A **358**, 145 (1997).
[6] J. K. Tuli, Nucl. Data Sheets **89**, 641 (2000).
[7] J. K. Hwang, A. V. Ramayya, J. H. Hamilton, L. K. Peker, J. Kormicki, B. R. S. Babu, T. N. Ginter, and C. J. Beyer, Phys. Rev. C **57**, 2250 (1998).
[8] A. Nowak, W. Urban, W. Kurcewicz, T. Rząca-Urban, H. Mach, B. Fogelberg, J. L. Durell, M. J. Leddy, M. A. Jones, W. R. Phillips, A. G. Smith, B. J. Varley, M. Bentaleb, E. Lubkiewicz, N. Schulz, I. Ahmad, and L. R. Morss, Eur. Phys J. A **6**, 1 (1999).
[9] M. P. Sadowski, M.Sc. thesis, Faculty of Physics, University of Warsaw, 2006 (unpublished).
[10] M. A. C. Hotchkis, J. L. Durell, J. B. Fitzgerald, A. S. Mowbray, W. R. Phillips, I. Ahmad, M. Carpenter, R. V. F. Janssens, T. L. Khoo, E. F. Moore, L. R. Morss, Ph. Benet, and D. Ye, Nucl. Phys. **A530**, 111 (1991).
[11] W. Urban, T. Rząca-Urban, J. L. Durell, A. G. Smith, and I. Ahmad, Phys. Rev. C **70**, 057308 (2004).
[12] W. Urban, T. Rząca-Urban, J. L. Durell, A. G. Smith, and I. Ahmad, Eur. Phys. J. A **24**, 161 (2005).
[13] W. Urban, Ch. Droste, T. Rząca-Urban, A. Złomaniec, J. L. Durell, A. G. Smith, B. J. Varley, and I. Ahmad, Phys. Rev. C **73**, 037302 (2006).
[14] W. Urban, M. A. Jones, J. L. Durell, M. J. Leddy, W. R. Phillips, A. G. Smith, B. J. Varley, I. Ahmad, L. R. Morss, M. Bentaleb, E. Lubkiewicz, and N. Schulz, Nucl. Phys. **A613**, 107 (1997).
[15] M. A. Jones, W. Urban, and W. R. Phillips, Rev. Sci. Instrum. **69**, 4120 (1998).

[16] S. Raman, C. H. Malarkey, W. T. Milner, C. W. Nestor Jr., and P. H. Stelson, At. Data Nucl. Data Tables **36**, 1 (1987).
[17] A. A. Sonzogni, Nucl. Data Sheets **93**, 599 (2001).
[18] E. Moll *et al.*, Kerntechnik **19**, 374 (1977).
[19] H. Wohlfarth, W. Lang, H. Dann, H.-G. Clerc, K.-H. Schmidt, and H. Schrader, Z. Phys. A **287**, 153 (1978).
[20] Y. Baudinet-Robinet, Phys. Rev. A **26**, 62 (1982).
[21] G. Duchene, F. A. Beck, P. J. Twin, G. de France, D. Curien, L. Han, C. W. Beausang, M. A. Bentley, P. J. Nolan, and J. Simpson, Nucl. Instrum. Methods B **90**, 432 (1999).
[22] T. Materna, A. Bail, L. Mathieu, U. Köster, H. Faust, O. Serot, and F. Michel-Sendis, AIP Conf. Proc. **1175**, 367 (2009).
[23] W. Urban, A. Korgul, T. Rząca-Urban, N. Schulz, M. Bentaleb, E. Lubkiewicz, J. L. Durell, M. J. Leddy, M. A. Jones, W. R. Phillips, A. G. Smith, B. J. Varley, I. Ahmad, and L. R. Morss, Phys. Rev. C **61**, 041301(R) (2000).
[24] G. S. Simpson, J. C. Angelique, J. Genevey, J. A. Pinston, A. Covello, A. Gargano, U. Köster, R. Orlandi, and A. Scherillo, Phys. Rev. C **76**, 041303(R) (2007).
[25] A. Złomaniec, H. Faust, J. Genevey, J. A. Pinston, T. Rząca-Urban, G. S. Simpson, I. Tsekhanovich, and W. Urban, Phys. Rev. C **72**, 067302 (2005).
[26] W. Urban, T. Rząca-Urban, J. L. Durell, W. R. Phillips, A. G. Smith, B. J. Varley, N. Schulz, and I. Ahmad, Phys. Rev. C **69**, 017305 (2004).
[27] M. Bentaleb, N. Schulz, E. Lubkiewicz, J. L. Durell, C. J. Pearson, W. R. Phillips, J. Shannon, B. J. Varley, I. Ahmad, C. J. Lister, L. R. Morss, K. L. Nash, and C. W. Williams, Z. Phys. A **354**, 143 (1996).
[28] W. Urban, N. Schulz, M. Bentaleb, E. Lubkiewicz, J. L. Durell, M. J. Leddy, M. A. Jones, W. R. Phillips, A. G. Smith, B. J. Varley, I. Ahmad, and L. R. Morss, Eur. Phys. J. A **8**, 5 (2000).
[29] T. Rząca-Urban, W. Urban, M. Saha Sarkar, S. Sarkar, J. L. Durell, A. G. Smith, B. J. Varley, and I. Ahmad, Eur. Phys. J. A **32**, 5 (2007).
[30] T. Rząca-Urban, K. Pgowska, W. Urban, A. Złomaniec, J. Genevey, J. A. Pinston, G. S. Simpson, M. Saha Sarkar, S. Sarkar, H. Faust, A. Scherillo, I. Tsekhanovich, R. Orlandi, J. L. Durell, A. G. Smith, and I. Ahmand, Phys. Rev. C **75**, 054319 (2007).
[31] P. Semmes and I. Ragnarsson (unpublished).
[32] C. Thibault, F. Touchard, S. Büttgenbach, R. Klapisch, M. De Saint Simon, H. T. Duong, P. Jacquinot, P. Juncar, S. Liberman, P. Pillet, J. Pinard, J. L. Vialle, A. Pesnelle, and G. Huber (Isolde Collaboration), Nucl. Phys. **A367**, 1 (1981).
[33] T. Bengtsson and I. Ragnarsson, Nucl. Phys. **A436**, 14 (1985).
[34] S. E. Larsson, G. A. Leander, and I. Ragnarsson, Nucl. Phys. **A307**, 189 (1978).
[35] J. A. Pinston, W. Urban, Ch. Droste, T. Rząca-Urban, J. Genevey, G. Simpson, J. L. Durell, A. G. Smith, B. J. Varley, and I. Ahmad, Phys. Rev. C **74**, 064304 (2006).
[36] G. A. Leander, W. Nazarewicz, P. Olanders, I. Ragnarsson, and J. Dudek, Phys. Lett. **B152**, 284 (1985).
[37] T. Rząca-Urban, W. Urban, J. A. Pinston, G. S. Simpson, J. L. Durell, A. G. Smith, and I. Ahmad, Phys. Rev. C (submitted).